RSC Advances

Preparation of highly controlled nanostructured Au within mesopores using reductive deposition in non-polar environments

Journal:	*RSC Advances*
Manuscript ID:	RA-ART-04-2014-003641.R1
Article Type:	Paper
Date Submitted by the Author:	30-May-2014
Complete List of Authors:	Kitahara, Masaki; Waseda University, Department of Applied Chemistry Kuroda, Kazuyuki; Waseda University, Department of Applied Chemistry

Journal Name

RSCPublishing

ARTICLE

Preparation of highly controlled nanostructured Au within mesopores using reductive deposition in non-polar environments

Cite this: DOI: 10.1039/xoxxoooooox

Received ooth January 2012,
Accepted ooth January 2012

DOI: 10.1039/xoxxoooooox

www.rsc.org/

Masaki Kitahara[a] and Kazuyuki Kuroda[*a, b]

This paper describes a sophisticated and unique method of Au deposition exclusively inside mesoporous silica, in clear contrast to general methods requiring surface modification with organic functional groups interacting with Au. Reductive deposition using hexane and 1,1,3,3-tetramethydisiloxane as solvent and reducing agent, respectively, was very successful in the inside deposition of Au in two-dimensional hexagonal mesoporous silica (SBA-15). This result was attributed to the suppression of migration of Au species (Au ions, atoms, and clusters) inside SBA-15 by forcibly locating Au species near the relatively polar mesopore surfaces in the presence of highly non-polar compounds in the mesochannels. Au nanorods replicated from the pore shape of SBA-15 were prepared by the reductive deposition, while Au nanoparticles were selectively formed by performing the deposition in the presence of hexadecyltrimethylammonium bromide, which shows promise in further development of precise design strategies for nanostructured Au.

Introduction

Nanostructured Au materials (nanoparticles, nanorods, and nanoplates) have attracted much attention because of their unique properties,[1] and many applications, such as catalysts,[2] sensors,[3,4] and colored materials,[5] among others. Because the properties of nanostructured Au are greatly influenced by their morphology and size on the nanometer-scale, precise control of morphology and size of nanostructured Au is essential for their applications.

Two major synthetic approaches to control the morphology and size of nanostructured Au are surfactant-assisted[1,6,7] and templating[8-27] methods. In the surfactant-assisted method, nanostructured Au is prepared by the anisotropic growth of Au crystals in the presence of surfactants or polymers. Although a simple and one-step process, this method does not offer precise control over the sizes of nanostructured Au. In contrast, a templating method using inorganic nanoporous materials as rigid frameworks can control the size and morphology of nanostructured Au by allowing for variations in both pore size and shape.

Among the various inorganic nanoporous materials employed for this purpose, mesoporous silica is particularly useful as a template because both pore size and shape can be precisely controlled,[28] which permits the preparation of nanostructured Au with controlled morphology and size. In addition, mesoporous silica is useful not only as a template but also as catalyst support owing to its chemical and thermal stabilities.[29] The use of mesoporous silica can suppress leaching and aggregation of Au nanoparticles during catalytic reactions. Because of the usefulness of mesoporous silica as both a template and catalyst support, numerous reports have described the preparation of nanostructured Au using mesoporous silica.[11-24,29]

For the preparation of nanostructured Au using mesoporous silica, Au deposition outside the mesoporous silica must be avoided. Au deposited on the outer surface of mesoporous silica tends to form bulk particles whose properties are completely different from those of nanostructured Au. Because it is difficult to separate formed bulk particles from the nanostructured Au, Au materials with suitable properties for desired applications cannot be obtained. Therefore, controlled Au deposition exclusively within the mesoporous silica framework is absolutely necessary for the preparation of nanostructured Au using mesoporous silica.

The mobilities of Au species (Au ions, atoms, and clusters) inside mesoporous silica are high because of their low affinities with the surface of mesoporous silica[30]; thus, it is necessary to introduce a Au precursor into mesopores, and furthermore, suppress the migration of Au species during the reductive deposition process. In most reports describing Au deposition inside mesoporous silica, silanol groups located on the surface are modified with organic groups which strongly interact with Au species to suppress their migration.[13,15-19,21,29] However, surface modification is undesirable for the following three reasons: 1) Both the amount and location of deposited Au depend on the amount and location of modified organic groups; the dense and homogeneous deposition of Au inside mesoporous silica remains difficult because homogeneous and high-density organic modifications are still challenging. 2) Removal of the modified organic groups by calcination is required to achieve a direct contact between Au and silica surfaces; however, this process induces the aggregation of Au nanoparticles. 3) Surface modification is a tedious process.

Although Au deposition inside mesoporous silica without surface modification has been reported, there are some drawbacks to these previously reported deposition methods as described below.[12,14,22-25] Thermal reduction at high temperature under H_2 flow is unfavorable from the viewpoint of energy consumption.[12,24,25] In addition, considering that the migration of Au species is enhanced at high temperature, it is unlikely that all Au is deposited inside mesoporous silica although the outside deposition is not fully discussed. Glow discharge plasma reduction requires reduced pressure and inert gas replacement.[14] UV reduction is undesirable from an environmental point of view because the method requires organic solvent vapor as a radical source.[25] Furthermore, these methods require special equipments, and large-scale preparation is difficult. Although electrodeposition is a mild and simple method that does not require special equipments,[22,23] the scale of preparation is quite small because the method is applicable only to mesoporous silica films on conductive substrates. Therefore, a more sophisticated deposition method capable of overcoming the issues as described above is highly demanded.

Here, we report the deposition of Au exclusively inside mesoporous silica by a liquid phase deposition process using a non-polar solvent and unique reducing agent. The method reported here has several advantages, including ease of scale-up, energy consumption, and simple synthetic equipments. Although liquid-phase deposition is an ideal process because of these advantages, this method is not suited to the templating method because Au precursors incorporated into the template tend to migrate outside the template owing to their dissolution into solvents containing reducing agents. Therefore, we have conceived a protocol employing a reducing agent/solvent combination, both of which have low affinity with the Au precursor, to enable Au deposition inside mesoporous silica. In this study, Au is exclusively deposited inside two-dimensional (2D) mesoporous silica (SBA-15)[31] without outside deposition by using hexane and 1,1,3,3-tetramethyldisiloxane. In addition, we have succeeded in separately preparing Au nanorods without simultaneous addition of surfactants and Au nanoparticles using (hexadecyltrimethylammonium bromide CTAB) as a surfactant. Because the properties of nanostructured Au are greatly influenced by their morphology and size, the utility of the method reported here becomes apparent since nanoparticles and nanorods can be selectively prepared by simply performing deposition in the presence or absence of the surfactants.

Experimental

Materials.

Tetraethoxysilane (TEOS, Tokyo Chemical Industry Co., Ltd.), triblock copolymer $EO_{20}PO_{70}EO_{20}$ (Pluronic 123, Aldrich Co.), and hydrochloric acid (35-37 wt%, Wako Pure Chemical Industries Ltd.) were used for the synthesis of SBA-15. $HAuCl_4{\cdot}4H_2O$ (Kanto Chemical Co., Inc.) was used as a Au precursor. Anhydrous ethanol (Wako Pure Chemical Industries Ltd.) was used as a solvent for incorporation of the Au precursor. Hexane (Wako Pure Chemical Industries Ltd.) and 1,1,3,3-tetramethyldisiloxane (TMDS, Tokyo Chemical Industry Co., Ltd.) were used as solvent and reducing agent, respectively. Hexadecyltrimethylammonium bromide (CTAB; Wako Pure Chemical Industries Ltd.) was used as a capping agent to control the morphology of the nanostructured Au inside mesoporous silica.

Synthesis of SBA-15.

Mesoporous silica SBA-15 was hydrothermally synthesized at 100 °C according to a literature.[31] Synthesized SBA-15 had a highly ordered 2D hexagonal mesostructure, as determined by its X-ray diffraction (XRD) pattern (Electronic Supporting Information (ESI), Figure S1). The unit cell parameter was calculated as 10.6 nm from the d_{10} spacing of the XRD pattern. Straight mesochannels were clearly observed in the transmission electron microscopy (TEM) image (ESI, Figure S2). The N_2 adsorption desorption isotherm of SBA-15 was typical type IV (ESI, Figure S3), which is characteristic of mesoporous materials. The pore size of SBA-15 as calculated by the Barrett-Joyner-Halenda (BJH) method was calculated as 8.1 nm (ESI, Figure S3, inset) and the pore volume was estimated as 1.2 cm^3/g from the volume of adsorbed N_2 at P/P_0 = *ca.* 0.99.

Preparation of Au nanorods inside SBA-15.

SBA-15 was dried under reduced pressure at 120 °C to remove adsorbed water. The dried SBA-15 (0.1 g) was then dispersed in anhydrous ethanol (10 mL). A stock solution of $HAuCl_4{\cdot}4H_2O$ in ethanol (12 μL, corresponding to 0.029 mmol of Au) was added to the solution containing SBA-15. The mixed solution was placed under reduced pressure to incorporate the Au precursor into the mesopores of SBA-15 by capillary forces; this process yielded a dried powder. The color of the Au-incorporated SBA-15 powder was yellow. After the powders were dispersed in hexane (5 mL), TMDS (103 μL, 0.58 mmol) was added to the hexane solution under stirring; the color of the powder was observed to change to black-purple within 1 min. After stirring for 1 h, the hexane solution was filtered. The obtained powders were washed with hexane and ethanol and dried at room temperature under an air atmosphere. The obtained product was denoted as SBA-15/Au.

Preparation of Au nanoparticles inside SBA-15 by adding hexadecyltrimethylammonium bromide (CTAB).

The preparative procedure of Au nanopaprticles inside SBA-15 was almost same except the addition of CTAB before the reduction. Before the addition of TMDS, CTAB (0.091 g, 0.25 mmol) was added into the solution. The color of the powders in the solution turned orange from yellow during stirring, which indicates the formation of a gold complex with CTAB.[32] After stirring for 1 h, the reducing agent was added into the mixture. The color of the powders in the solution turned from orange to purple. After stirring for 1 h, the hexane solution was filtered. The obtained powders were washed with hexane and ethanol and dried at room temperature in air atmosphere. The obtained product was denoted as SBA-15/Au_CTAB

Characterization.

TEM images, selected area electron diffraction (SAED) patterns, and energy dispersive X-ray (EDX) spectra were recorded on a JEOL JEM-2010 electron microscope (accelerating voltage of 200 kV). Samples were dispersed in ethanol and mounted on a STEM microgrid for TEM observations. High-angle XRD patterns were measured using a Rigaku RINT-Ultima III diffractometer with a high-speed X-ray detector (D/teX Ultra; Cu Kα radiation of 40 kV, 40 mA). Low-angle XRD patterns were measured using a Rigaku Ultima IV diffractometer (Fe Kα radiation of 40 kV, 30 mA). N_2 adsorption-desorption isotherms were measured using a Quantachrome Autosorb-1 apparatus. The sample was preheated at 120 °C for 3 h under vacuum. Pore size

distributions were calculated from the adsorption branch by the BJH method. Solid-state ^{29}Si magic-angle spinning (MAS) NMR measurement was recorded using a JEOL JNM-CMX-400 spectrometer at a resonance frequency 79.42 MHz with a pulse width of 45° and a recycle delay of 100s. Chemical shifts for ^{29}Si MAS NMR were referenced to poly(dimethylsilane) at -33.8 ppm. FT-IR spectra were recorded on a JASCO FT/IR 6100 spectrometer by a KBr disk technique.

Results

Characterization of SBA-15/Au.

The TEM images of SBA-15/Au are shown in Figure 1a and 1b. A rod-like morphology replicated from the cylinder-like pore of SBA-15 was observed along the mesopores of SBA-15. The diameter of the nanorods was estimated to be about 8 nm, corresponding to the pore size of SBA-15. These results show that Au was deposited inside the mesopores of SBA-15. Furthermore, it should be noted that almost no particles other than nanorods were observed even in the low-magnified TEM image (Figure 1a), indicating that single-phase Au nanorods were obtained.

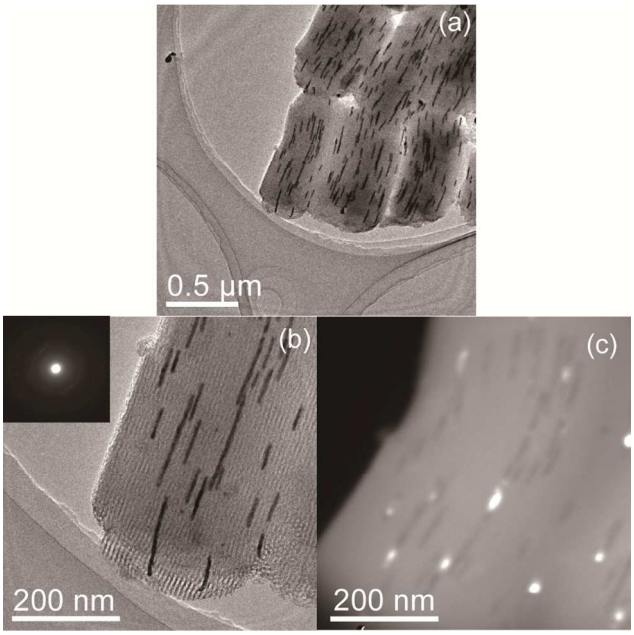

Figure 1 TEM images of SBA-15/Au (a) low-magnification, (b) high magnification (inset: corresponding SAED pattern) and (c) dark-field TEM image in the same area as b.

The SAED pattern (Figure 1b, inset) showed ring-like diffractions, although the intensity of the diffractions was very weak. This weak intensity can be explained by both the small amount of Au in the area and electron-beam scattering by mesoporous silica. The single-crystalline domain size of the Au nanorods was estimated to be less than 30 nm as determined from dark-field TEM image (Figure 1c), which was smaller than the long-axis length (several tens of nm to *ca.* 200 nm); these data are indicative of the polycrystalline nature of the Au nanorods. As determined from the (111) lattice plane in the XRD pattern of SBA-15/Au (Figure 2), the crystallite size was calculated as *ca.* 16 nm by the Scherrer equation using the Scherrer constant K = 1. This calculated value is close to that estimated from the dark-field TEM image, which suggests that Au nanorods were formed inside SBA-15/Au without the accompanying formation of bulk Au particles. After the reduction, silanol groups located on the surface of SBA-15 were modified with TMDS at least partly, which is supported by the reduction of the signal due to Q^3 units of SBA-15 and the presence of signals due to M and D units of TMDS (ESI, Figure S4). Three bands at 2924 cm^{-1} (CH_3 sym stretching), 2853 cm^{-1} (CH_3 asym stretching), and 2148 cm^{-1} (Si-H stretching) were observed in the FT-IR spectrum of SBA-15/Au (ESI, Figure S5), also supporting the surface modification with TMDS.

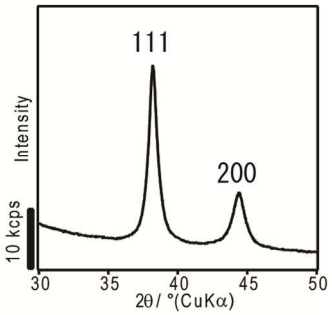

Figure 2 XRD pattern of SBA-15/Au.

Characterization of SBA-15/Au_CTAB.

The liquid-phase deposition process has advantages from the viewpoint of the control of reductive behavior using capping agents, such as surfactants and polymers. This controllability is important for preparation of nanostructured Au because reductive behavior is strongly related to the morphology and size of deposited Au inside mesoporous silica. Therefore, we added CTAB, often used as a capping agent for preparation of nanostructured Au in a liquid phase, [1,6,7] to the hexane solution prior to reduction.

The TEM image of SBA-15/Au_CTAB is shown in Figure 3a. The removal of CTAB molecules was confirmed by EDX spectra of SBA-15/Au_CTAB before and after washing (ESI, Figure S6 and Figure 3b, respectively), showing the absence of bromide and chloride ions after washing. Au nanoparticles were observed with morphologies noticeably different from the Au nanorods prepared without CTAB. In addition, the formed Au nanoparticles had a noticeably wider distribution than Au nanorods, although accurate three-dimensional distributions could not be obtained from the TEM images. The diameters of the nanoparticles were *ca.* 8 nm, almost identical to the pore size of SBA-15. Outer deposition of Au was not observed even in the low-magnified TEM image (ESI, Figure S7) as well as SBA-15/Au. The crystallite size was calculated as about 8 nm from the (111) lattice plane in the XRD pattern (Figure 4) using the Scherrer equation, indicating that each Au nanoparticle was single crystalline. In contrast, when the amount of CTAB was decreased, not only nanoparticles but also nanorods were observed (ESI, Figure S8). These data show that CTAB changed the morphology of nanostructured Au inside mesoporous silica; the reason for this morphological variation by the addition of CTAB is discussed in the next section.

We have already reported the preparation of nanostructured Pt using a mesoporous silica film in the presence of surfactant molecules using an electrodeposition process.[33] Although electrodeposition is suitable for metal deposition within mesopores in a liquid phase because the deposition site is limited to the surface of substrate, a conductive substrate is necessary for successful preparation. Conversely, the deposition method using a chemical reducing agent reported here is advantageous in terms of its applicability to not only powders but also films on insulating substrates.

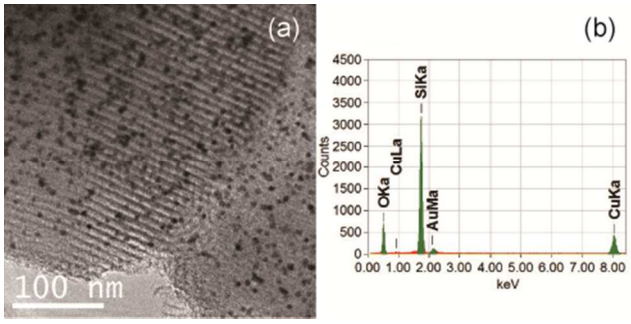

Figure 3 (a) TEM image of SBA-15/Au_CTAB and (b) corresponding EDX spectrum.

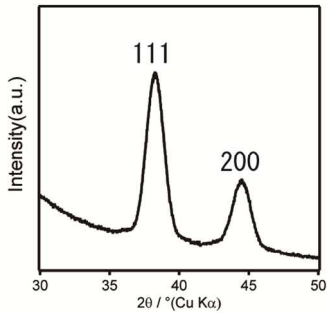

Figure 4 XRD pattern of SBA-15/Au_CTAB.

Discussion

Significance of the use of non-polar compounds as a solvent and a reducing agent.

In this study, we have succeeded in performing Au deposition solely inside mesoporous silica without surface modification. The most significant difference between the preparative method reported here and those in previous reports is the use of non-polar-liquid as a medium for reductive deposition. Therefore, this difference is strongly related to successful Au deposition.

In order to deposit Au inside mesoporous silica, the migration of Au species must be suppressed. Au species migrate inside mesoporous silica either by pore surface diffusion or pore bulk diffusion; pore surface diffusion is the dominant migration mechanism for compounds interacting with the surface of mesoporous silica, whereas pore bulk diffusion predominates for compounds that do not interact with the surface.[34] The diffusion coefficient of pore surface diffusion is much smaller than that of pore bulk diffusion.[34,35] In addition, stronger interactions will lead to slower pore surface diffusion.[36] Therefore, it is vital to promote stronger interactions of Au species with mesopore surfaces in order to suppress the migration of Au species.

In the initial reduction process, Au precursors and partially reduced precursors, both of which are ionic compounds, exist within the mesopores. The ionic Au compounds interact with the silica surfaces owing to the presence of polar silanol groups. In particular, because hexane has a low affinity with the ionic Au compounds, these species should be located near the surface in the hexane solution; this suggests that the use of hexane leads to the restriction of the Au species migration by pore surface diffusion which is much slower than pore bulk diffusion[34]-one of roles of hexane for controlled Au deposition inside mesoporous silica. Because the interactions between polar compounds increase inversely with the dielectric constant of the reaction medium, it is reasonable to suggest that the use of solvent with extremely low dielectric constant such as hexane suppresses migration. Outer deposition of Au was slightly observed when other reducing agents, like triethyl-, butyl-, and hexyl-silanes were used for the deposition (ESI, Figure S9). The use of triphenylsilane induced larger outer deposition of Au. The function of reducing agent in the non-polar systems needs further studies.

With the progress of the reduction process, Au atoms or clusters, which are no longer ionic compounds, are formed within the mesopores. As a result of the weak interactions between silanol groups and Au,[30] Au atoms or clusters should migrate not only by pore surface diffusion but also pore bulk diffusion.[34] Although this is not related to the state (liquid or gas) of the reductive reaction medium, the diffusion coefficient for pore bulk diffusion in the liquid phase is smaller than that in the gas phase by two to three orders of magnitude.[35] This means that the use of liquid hexane as the reductive reaction medium suppresses the migration of Au species compared to the gas phase.

Effect of the addition of CTAB.

As shown in the Results section, the addition of CTAB into the hexane solution before reduction resulted in the formation of Au nanoparticles within the mesopores. Here, the effect of the addition of CTAB is discussed. CTAB forms complexes with $HAuCl_4$ (CTA-$AuBr_4$),[32] and is known to strongly interact with Au atoms and clusters.[1,6,7] Therefore, the apparent sizes of Au species are presumed to enlarge further in the presence of CTAB than in the absence of CTAB, which should suppress the migration of Au species within the mesopores. As previously demonstrated, because the molecular size of CTAB is comparative to the complementary pores,[31] migration between the mesopores through these pores should be suppressed. This naturally disturbs the crystal growth or aggregation of Au, resulting in the formation of Au nanoparticles.

Conclusion

In this study, we have demonstrated that the use of non-polar liquid as a solvent and reducing agent is valuable for controlled Au deposition exclusively inside mesoporous silica. Hexane and reducing agent TMDS play critical roles in suppressing the migration of Au species within the mesopores. In addition, we have succeeded in the selective preparation of Au nanoparticles and nanorods by simply performing reductive deposition in the presence or absence of CTAB. The use of surfactants such as CTAB for the hard templating method is advantageous for the liquid phase deposition process reported here, which enables further precise design of nanostructured Au materials. More importantly, the hard templating method using the liquid phase deposition process is expected to be applicable to not only mesoporous silica and Au but also various nanoporous materials and metal species. In particular, this method would be useful for deposition inside nanoporous materials with low thermal stability, such as metal-organic frameworks (MOFs)[37] and porous coordination polymers (PCP)[38], via facile metal deposition under very mild conditions.

Acknowledgements

We would like to acknowledge Mr. M. Fuziwara (Waseda University) for his kind assistance in TEM observations, Mr. T. Sakakibara (Department of Applied Chemistry, Waseda University) for experimental supports, and Ms. M. Tamai (Department of Applied Chemistry, Waseda University) for the measurement of ^{29}Si MAS NMR. This work was supported by a Grant-in-Aid for Scientific Research (No. 23245044). M.K

thanks for Japan Chemical Industry Association for a fellowship (Human Resources Fostering Program in Chemistry).

Notes and references

[a] Department of Applied Chemistry, Faculty of Science and Engineering, Waseda University, Ohkubo 3-4-1, Shinjuku-ku, Tokyo, 169-8555, Japan.
[b] Kagami Memorial Research Institute for Materials Science and Technology, Waseda University, Nishiwaseda 2-8-26, Shinjuku-ku, Tokyo, 169-0051, Japan.
E-mail: kuroda@waseda.jp; Fax: +81-3-5286-3199; Tel: +81-3-5286-3199

† Electronic Supplementary Information (ESI) available: [Figure S1 XRD pattern of SBA-15, Figure S2 TEM image of SBA-15, Figure S3 N_2 adsorption desorption isotherm of SBA-15 (inset: BJH pore size distribution), Figure S4 ^{29}Si MAS NMR spectrum of SBA-15/Au, Figure S5 FT-IR spectra of SBA-15 and SBA-15/Au, Figure S6 EDX spectrum of SBA-15_CTAB prepared without washing with hexane and ethanol, Figure S7 Low-magnified TEM image of SBA-15/Au_CTAB, Figure S8 TEM image of SBA-15/Au_CTAB prepared by the reduction in the presence of 0.025 mmol of CTAB, Figure S9 TEM images of SBA-15/Au prepared by using (a) triethylsilane, (b) tributylsilane, (c) trihexylsilane, and (d) triphenylsilane as reducing agents, respectively.]. See DOI: 10.1039/b000000x/

1 Y. Xia, Y. Xiong, B. Lim and S. E. Skrabalak, *Angew. Chem. Int. Ed.*, 2009, **48**, 60-103.
2 M. Haruta, *Gold Bull.*, 2004, **37**, 27-36.
3 K. M. Mayer and J. H. Hafner, *Chem. Rev.*, 2011, **111**, 3828-3857.
4 K. Saha, S. S. Agasti, C. Kim, X. Li and V. M. Rotello, *Chem. Rev.*, 2012, **112**, 2739-2779.
5 S. Link and M. A. El-Sayed, *Annu. Rev. Phys. Chem*, 2003, **54**, 331-366.
6 T. H. Tran and T. D. Nguyen, *Colloids Surf., B*, 2011, **88**, 1-22.
7 S. E. Lohse and C. J. Murphy, *Chem. Mater.*, 2013, **25**, 1250-1261.
8 C. A. Foss Jr, G. L. Hornyak, J. A. Stockert and C. R. Martin, *J. Phys. Chem.*, 1994, **98**, 2963-2971.
9 M. S. Sander and L. S. Tan, *Adv. Funct. Mater.*, 2003, **13**, 393-397.
10 Y. Kuroda and K. Kuroda, *Angew. Chem. Int. Ed.*, 2010, **49**, 6993-6997.
11 Y. Kuroda, Y. Sakamoto and K. Kuroda, *J. Am. Chem. Soc.*, 2012, **134**, 8684-8692.
12 Y. J. Han, J. M. Kim and G. D. Stucky, *Chem. Mater.*, 2000, **12**, 2068-2069.
13 A. Takai, Y. Doi, Y. Yamauchi and K. Kuroda, *J. Phys. Chem. C*, 2010, **114**, 7586-7593.
14 Z. J. Wang, Y. Xie and C. J. Liu, *J. Phys. Chem. C*, 2008, **112**, 19818-19824.
15 Y. Xie, S. Quinlivan and T. Asefa, *J. Phys. Chem. C*, 2008, **112**, 9996-10003.
16 Z. Li, C. Kübel, V. I. Pârvulescu and R. Richards, *ACS Nano*, 2008, **2**, 1205-1212.
17 N. Petkov, N. Stock and T. Bein, *J. Phys. Chem. B*, 2005, **109**, 10737-10743.
18 C. M. Yang, H. S. Sheu and K. J. Chao, *Adv. Funct. Mater.*, 2002, **12**, 143-148.
19 J. Gu, J. Shi, Z. Hua, L. Xiong, L. Zhang and L. Li, *Chem. Lett.*, 2005, **34**, 114-115.
20 Y. Zhang, A. H. Yuwono, J. Li and J. Wang, *Microporous Mesoporous Mater.*, 2008, **110**, 242-249.
21 J. Gu, J. Shi, L. Xiong, H. Chen, L. Li and M. Ruan, *Solid State Sci.*, 2004, **6**, 747-752.
22 Y. Kanno, T. Suzuki, Y. Yamauchi and K. Kuroda, *J. Phys. Chem. C*, 2012, **116**, 24672-24680.
23 Y. Kanno and K. Kuroda, *Bull. Chem. Soc. Jpn.*, 2013, **86**, 583-585.
24 A. Fukuoka, T. Higuchi, T. Ohtake, T. Oshio, J. I. Kimura, Y. Sakamoto, N. Shimomura, S. Inagaki and M. Ichikawa, *Chem. Mater.*, 2006, **18**, 337-343.
25 H. Araki, A. Fukuoka, Y. Sakamoto, S. Inagaki, N. Sugimoto, Y. Fukushima and M. Ichikawa, *J. Mol. Catal. A: Chem.*, 2003, **199**, 95-102.
26 J. K. Song, U. H. Lee, H. R. Lee, M. Suh and Y. U. Kwon, *Thin Solid Films*, 2009, **517**, 5705-5709.
27 M. D. Pérez, E. Otal, S. A. Bilmes, G. J. A. A. Soler-Illia, E. L. Crepaldi, D. Grosso and C. Sanchez, *Langmuir*, 2004, **20**, 6879-6886.
28 Y. Wan and D. Zhao, *Chem. Rev.*, 2007, **107**, 2821-2860.
29 L.-F. Gutiérrez, S. Hamoudi and K. Belkacemi, *Catalysts*, 2011, **1**, 97-154.
30 A. Kulkarni, R. J. Lobo-Lapidus and B. C. Gates, *Chem. Commun.*, 2010, **46**, 5997-6015.
31 A. Galarneau, H. Cambon, F. Di Renzo, R. Ryoo, M. Choi and F. Fajula, *New J. Chem.*, 2003, **27**, 73-79.
32 Z. J. Lin, X. M. Chen, Z. M. Cai, M. Oyama, X. Chen and X. R. Wang, *Cryst. Growth Des.*, 2008, **8**, 863-868.
33 A. Takai, H. Ataee-Esfahani, Y. Doi, M. Fuziwara, Y. Yamauchi and K. Kuroda, *Chem. Commun.*, 2011, **47**, 7701-7703.
34 D. Weber, A. J. Sederman, M. D. Mantle, J. Mitchell and L. F. Gladden, *PCCP*, 2010, **12**, 2619-2624.
35 K. Miyabe and G. Guiochon, *J. Chromatogr. A*, 2010, **1217**, 1713-1734.
36 B. E. Feller, J. T. Kellis, L. G. Cascão-Pereira, C. R. Robertson and C. W. Frank, *Langmuir*, 2010, **26**, 18916-18925.
37 H. Furukawa, K. E. Cordova, M. O'Keeffe and O. M. Yaghi, *Science*, 2013, **341**.
38 S. Kitagawa, R. Kitaura and S. I. Noro, *Angew. Chem. Int. Ed.*, 2004, **43**, 2334-2375.